Worcester, MA, USA.
11. S. Munro and H. R. B. Pelham, *Cell* **48**, 899 (1987).
12. N. J. Bulleid and R. B. Freedman, *Nature* **335**, 649 (1988).
13. R. Noiva and W. J. Lennarz, *J. Biol. Chem.* **267**, 3553 (1992).
14. R. B. Freedman, T. R. Hirst, M. F. Tuite, *Trends Biochem. Sci.* **19**, 331 (1994).
15. L. G. Franzén, J.-D. Rochaix, G. von Heijne, *FEBS Lett.* **260**, 165 (1990).
16. K. Keegstra and L. J. Olsen, *Annu. Rev. Plant Physiol. Plant Mol. Biol.* **40**, 471 (1989).
17. An immunoblot analysis of isolated chloroplasts from *C. reinhardtii* cells was performed with both antisera to tubulin and *C. reinhardtii* RB60. Although a specific 60-kD band was detected in isolated *C. reinhardtii* chloroplasts, it was not possible to obtain pure chloroplasts free of cytoplasmic proteins by density gradient centrifugation because of the similar density of whole cells and isolated chloroplasts. We therefore used pea chloroplasts for this assay, which can be readily obtained in pure form by Percoll gradient centrifugation.
18. Full-length r-RB47 is 69 kD and contains a COOH-terminal domain that is cleaved in vivo to yield the native 47-kD protein (*8*). To generate the endogenous form of RB47, we mapped the location of the 47-kD polypeptide on the full-length recombinant protein by comparing mass spectrometric data of tryptic digests of the *C. reinhardtii* 47-kD protein with the full-length recombinant protein. These data showed that the 47-kD protein encompasses the four RNA recognition motif domains found in all polyadenylate [poly(A)]-binding proteins, but lacked the COOH-terminal portion of the protein.
19. To examine whether auto-phosphorylation of r-RB60 could affect the binding of r-RB47 to the 5′-UTR of *psbA* mRNA, we incubated r-RB47 and r-RB60 in the presence or absence of 3 mM ATP followed by gel mobility-shift assay. The RNA binding activity of r-RB47 was not altered by the addition of ATP, showing that auto-phosphorylation of r-RB47 or r-RB60 is not responsible for reducing r-RB47 RNA binding.
20. J. Lundström and A. Holmgren, *J. Biol. Chem.* **265**, 9114 (1990).
21. C. R. Staples *et al.*, *Biochemistry* **35**, 11425 (1996).
22. S. P. Mayfield, C. B. Yohn, A. Cohen, A. Danon, *Annu. Rev. Plant Physiol. Plant Mol. Biol.* **46**, 147 (1995).
23. C. Robinson, in *Plant Cell Biology, A Practical Approach*, N. Harris and K. J. Oparka, Eds. (Oxford Univ. Press, Oxford, 1994), pp. 273–276.
24. We thank R. Beachy, A. Cohen, and R. Bruick for critical reading of the manuscript; A. Cohen for help with fast protein liquid chromatography; and B. Huang for anti-tubulin. Supported by grants from the NIH (GM54659) and the U.S. Department of Energy (DE-FG03-93ER70116) to S.P.M. J.K. is supported by a Skaggs Institute postdoctoral fellowship.

11 August 1997; accepted 31 October 1997

Sequence-Specific and Phosphorylation-Dependent Proline Isomerization: A Potential Mitotic Regulatory Mechanism

Michael B. Yaffe,* Mike Schutkowski,* Minhui Shen,* Xiao Zhen Zhou, P. Todd Stukenberg, Jens-Ulrich Rahfeld, Jian Xu, Jian Kuang, Marc W. Kirschner, Gunter Fischer, Lewis C. Cantley, Kun Ping Lu†

Pin1 is an essential and conserved mitotic peptidyl-prolyl isomerase (PPIase) that is distinct from members of two other families of conventional PPIases, cyclophilins and FKBPs (FK-506 binding proteins). In response to their phosphorylation during mitosis, Pin1 binds and regulates members of a highly conserved set of proteins that overlaps with antigens recognized by the mitosis-specific monoclonal antibody MPM-2. Pin1 is here shown to be a phosphorylation-dependent PPIase that specifically recognizes the phosphoserine-proline or phosphothreonine-proline bonds present in mitotic phosphoproteins. Both Pin1 and MPM-2 selected similar phosphorylated serine-proline–containing peptides, providing the basis for the specific interaction between Pin1 and MPM-2 antigens. Pin1 preferentially isomerized proline residues preceded by phosphorylated serine or threonine with up to 1300-fold selectivity compared with unphosphorylated peptides. Pin1 may thus regulate mitotic progression by catalyzing sequence-specific and phosphorylation-dependent proline isomerization.

Proline-directed protein kinases, such as cyclin-dependent protein kinases, play important roles in regulating eukaryotic cell division (*1*). At the G_2-to-M phase transition of the cell cycle, a rapid increase in Cdc2 kinase activity results in phosphorylation of many proteins on serine or threonine residues that are followed by proline (S/T–P sites) (*2*). Phosphorylation of these proteins is thought to trigger many of the structural modifications that occur during mitosis (*1–3*). However, it is not clear how this abrupt change in phosphorylation state leads to an organized and programmed set of mitotic events.

Pin1, originally isolated as a protein that interacts with and inhibits the essential mitotic kinase NIMA, is highly conserved and possesses both a WW domain and PPIase activity (*4*). PPIases catalyze the relatively slow peptidyl-prolyl isomerization of proteins, allowing relaxation of local energetically unfavorable conformational states (*5*). The cyclophilins and FKBPs, two major families of PPIases, are targets of clinically relevant immunosuppressive drugs. However, the immunosuppressive activity of these drugs is unrelated to inhibition of PPIase activity, and neither cyclophilin nor FKBP genes are essential (*5*). Thus, evidence for the biological importance of this enzymatic activity is limited.

In contrast, Pin1, a member of a family of PPIases that differ from cyclophilins and FKBPs, is essential for cell growth and requires a catalytically competent PPIase domain (*4*, *6*). Pin1 both negatively regulates entry into mitosis and is required for normal progression through mitosis in human cells and yeast (*4*). We have recently shown that Pin1 specifically interacts with and regulates the activity of a subset of mitotic proteins in a phosphorylation-dependent manner (*7*). However, little is known about how these specific interactions are achieved.

To investigate the mechanism by which Pin1 interacts with essential mitotic proteins, we used a glutathione S-transferase (GST)–Pin1 fusion protein to screen oriented degenerate peptide libraries (*8*). The crystal structure of Pin1 containing an Ala-Pro dipeptide substrate revealed a sulfate ion located 5 Å from the C_β carbon of Ala, suggesting that phosphorylated Ser (pS) might be preferred at this site (*9*). To test this idea, we prepared a pS-containing degenerate peptide library of general sequence H_2N-MAXXXpSXXXAKK, where X is any amino acid except Cys (*8*). The GST-Pin1 protein preferentially bound a subset of peptides with Pro immediately COOH-terminal to pS (Fig. 1A).

M. B. Yaffe, Division of Signal Transduction, Department of Medicine and Department of Surgery, Beth Israel Deaconess Medical Center, Boston, MA 02215, USA.
M. Schutkowski, J.-U. Rahfeld, G. Fischer, Max-Planck Research Unit on Enzymology of Protein Folding, Kurth-Mothes Strasse 3, 06120 Halle, Germany.
M. Shen and X. Z. Zhou, Cancer Biology Program, Division of Hematology and Oncology, Department of Medicine, Beth Israel Deaconess Medical Center, Boston, MA 02215, USA.
P. T. Stukenberg and M. W. Kirschner, Department of Cell Biology, Harvard Medical School, Boston, MA 02115, USA.
J. Xu, Division of Signal Transduction, Department of Medicine, Beth Israel Deaconess Medical Center, Boston, MA 02215, USA.
J. Kuang, Department of Clinical Investigation, University of Texas M.D. Anderson Cancer Center, Houston, TX 77030, USA.
L. C. Cantley, Division of Signal Transduction, Department of Medicine, Beth Israel Deaconess Medical Center, and Department of Cell Biology, Harvard Medical School, Boston, MA 02115, USA.
K. P. Lu, Cancer Biology Program, Division of Hematology/Oncology, Department of Medicine, Beth Israel Deaconess Medical Center, and Division on Aging, Harvard Medical School, 330 Brookline Avenue, HIM 1047, Boston, MA 02215, USA.

*These authors contributed equally to this work.
†To whom correspondence should be addressed. E-mail: klu@bidmc.harvard.edu

To investigate whether peptides containing pS-P were preferred substrates for the isomerase activity of Pin1, we synthesized oligopeptide substrates and assayed for cis-trans isomerization by Pin1 and by members of the cyclophilin (Cyp18) and FKBP (FKBP12) families of PPIases (*10*). Neither Cyp18 nor FKBP12 effectively catalyzed isomerization of peptides with pS/pT–P moieties (Table 1). In contrast, both Y-P and pY-P bonds were good substrates for both enzymes. Thus, phosphorylation of S/T–P, but not Y-P, renders the prolyl-peptidyl bond resistant to the catalytic action of conventional PPIases, suggesting the need for a different enzyme to catalyze this reaction.

In contrast to that of cyclophilins and FKBPs, the isomerase activity of Pin1 was highly specific for peptides with pS/pT–P bonds. Whereas Pin1 exhibited little isomerase activity with substrates containing S/T–P bonds, phosphorylation of these peptides on Ser or Thr resulted in up to a 300-fold increase in k_{cat}/K_m (Table 2). Pin1 showed low isomerization activity with peptides containing an A-P peptide bond; incorporation of Glu or Asp immediately preceding Pro in order to mimic pS increased isomerization activity. Peptides containing Y or pY preceding Pro were poor substrates for Pin1. This substrate specificity distinguishes Pin1 from the conventional PPIases in the cyclophilin and FKBP families.

To define further the sequence specificity of Pin1, we used a degenerate peptide library containing a fixed pS-P sequence flanked by three degenerate positions on each side. Pin1 selected Arg or aromatic residues at the −1 and +1 positions of the pS-P motif (Table 3). Aromatic amino acids were also selected at the −3 position, Phe or Ile at the −2 position, and Leu or Ile at the +2 position. On this basis, several additional peptides were synthesized as Pin1 substrates (*10*). Peptides with Arg introduced at the P+1 position proved more effective substrates, with k_{cat}/K_m values up to 1300 times those of their nonphosphorylated counterparts (Table 2). Placing aromatic residues NH_2-terminal to the pS-P position further improved these peptides as substrates (Table 2). The best substrate identified thus far (WFYpSPR-*p*NA) is the optimal sequence selected from the peptide library (Tables 2 and 3). The apparent

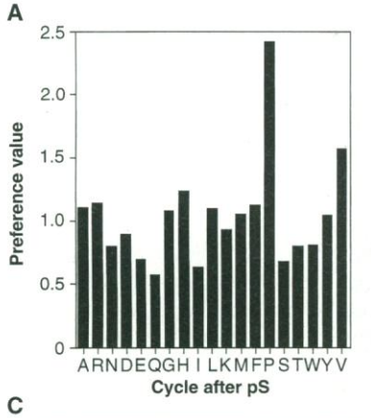

C

	k_{cat}/K_m(mM-1 s-1)	
	AASPR-*p*NA	AApSPR-*p*NA
Pin1	7	19,400
Pin1(R68,69A)	7	36
Pin1(H59A)	<1	1,120
Parvulin	520	<1

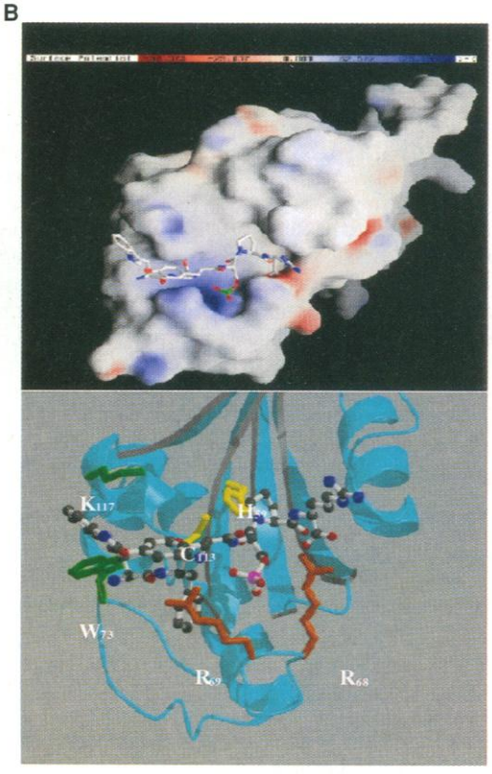

Fig. 1. Pin1 binding specificity and its structural basis. (**A**) Preference of Pin1 for peptides containing Pro immediately downstream of pS. GST-Pin1 was used to screen a peptide library of general sequence H_2N-MAXXXpSXXXAKK, where X is any amino acid except Cys, and the bound peptides were sequenced. Values indicate the relative abundance of each of the 19 amino acids at the sequencing cycle corresponding to the position immediately downstream of pS compared with their abundance in the starting library mixture. Abbreviations for the amino acid residues are as follows: A, Ala; C, Cys; D, Asp; E, Glu; F, Phe; G, Gly; H, His; I, Ile; K, Lys; L, Leu; M, Met; N, Asn; P, Pro; Q, Gln; R, Arg; S, Ser; T, Thr; V, Val; W, Trp; and Y, Tyr. (**B**) Molecular modeling of the optimal WFYpSPR peptide bound to Pin1. (Top) The molecular surface shaded by surface electrostatic potential shows the aromatic NH_2-terminus of the peptide in a hydrophobic channel, the pS phosphate in a basic pocket of R68 and R69, and the aliphatic Pro side chain within the hydrophobic cluster of L122, M130, and F134. The ω angle of the pS-P peptide bond is 90°. The surface potential ranges from −58.073 (dark red) to −29.037 (light red) to 0 (white) to 62.582 (light purple) to 125.165 (dark purple). (Bottom) Pin1 secondary structure showing selected residues. R68 and R69 coordinate the phosphate group (orange), C113 and H59 are implicated in the isomerization mechanism (yellow), and W73 and K117 participate in stacking the peptide Trp residue (green). (**C**) Isomerase activity of Pin1 and its mutants, expressed and purified as GST fusion proteins, compared with that of parvulin punified from *Escherichia coli*. Activity was assayed as described in Table 1.

Table 1. Failure of cyclophilin (Cyp18) and FKBP12 to catalyze effectively the isomerization of the pS/pT–P peptide bond. The assay was performed with purified proteins in triplicate by monitoring the absorbance of released 4-nitroaniline (*p*NA) with the use of chymotrypsin as an isomer-specific protease.

Substrate	Cyp18 k_{cat}/K_m ($mM^{-1}s^{-1}$)	FKBP12 k_{cat}/K_m ($mM^{-1}s^{-1}$)
AASPF-*p*NA	5400	29
AApSPF-*p*NA	50	1
AATPF-*p*NA	5200	27
AApTPF-*p*NA	9	2
Ac-AYPY-*p*NA	2420	880
Ac-ApYPY-*p*NA	3270	64
Ac-AEPF-*p*NA	2100	2

Table 2. Sequence-specific and phosphorylation-dependent PPIase activity of Pin1. Assays were performed as described in Table 1, with the exception that trypsin replaced chymotrypsin as an isomer-specific protease when peptides with Pro-Arg-*p*NA sequences were used as substrates.

Substrate	k_{cat}/K_m ($mM^{-1}s^{-1}$)
Suc-AAPL-*p*NA	55
Suc-AAPR-*p*NA	121
Suc-AAPM-*p*NA	134
Suc-ADPY-*p*NA	220
Suc-AEPF-*p*NA	3,410
Ac-AYPY-*p*NA	5
Ac-ApYPY-*p*NA	3
Ac-ASPY-*p*NA	269
Ac-ApSPY-*p*NA	3,370
Ac-ATPY-*p*NA	635
Ac-ApTPY-*p*NA	2,480
AAEPF-*p*NA	220
AASPF-*p*NA	9
AApSPF-*p*NA	3,760
AATPF-*p*NA	4
AApTPF-*p*NA	1,370
Ac-AASPR-*p*NA	7
Ac-AApSPR-*p*NA	9,300
Ac-AApTPR-*p*NA	3,700
WYpSPRT-*p*NA	14,100
WFYSPR-*p*NA	170
WFYpSPR-*p*NA	20,160

Michaelis constant (K_m) of Pin1 for this peptide was 10 μM (*10*).

Pin1 binds a large subset of mitotic phosphoproteins that are recognized by the monoclonal antibody MPM-2 (*7*) (Fig. 2A). We therefore investigated the sequence specificity for MPM-2 recognition. When immobilized MPM-2 antibody was used to probe a peptide library containing only pS as the orienting residue (*8*), peptides with Pro at the pS+1 position were preferentially selected (*11*). With the pS-P degenerate peptide library, MPM-2 preferentially selected peptides with aromatic or aliphatic amino acids at the −3, −1, and +1 positions relative to pS-P (Table 3). This MPM-2 binding motif is similar to the sequence motif selected by Pin1 (Table 3) and explains the observation that Pin1 specifically interacts with MPM-2 antigens (*7*).

The structural basis for Pin1 substrate specificity was investigated by molecular model-building and site-directed mutagenesis. On the basis of the Pin1-substrate crystal structure determined by Ranganathan *et al.* (9), the optimal peptide (WFYpSPR) was modeled onto the Pin1 structure, with the assumption that the phosphate group of pS occupies the position of sulfate in the previous structure (*12*) (Fig. 1B). In this model, R68 and R69 of Pin1 coordinate the pS phosphate, a hydrophobic groove accepts the preceding aromatic tripeptide, and the side chain of C113 and H59 coordinate the isomerizing pS-P peptide bond with an ω angle of 90°, stabilizing the transition state between the cis and trans configurations. To test these predictions, we generated site-specific Pin1 mutants and assayed their PPIase activity (*13*).

Substitution of both R68 and R69 by Ala reduced the k_{cat}/K_m for the phosphorylated substrate by a factor of ~500 relative to that of the wild-type enzyme (Fig. 1C). The catalytic activity of this mutant was identical to that of wild-type Pin1 with the unphosphorylated peptide substrate. Thus, this cluster of basic residues appears to participate in coordinating the phosphate of pS or pT. In parvulin (6), the prototype of the Pin1 family of PPIases, R68 and R69 of Pin1 are replaced by Glu; this enzyme failed to catalyze the isomerization of pS-P peptidyl bonds, although it was effective in catalyzing Pro isomerization in the unphosphorylated peptide (Fig. 1C). Replacement of the catalytic H59 residue of Pin1 with Ala markedly reduced PPIase activity toward both phosphorylated and unphosphorylated peptides (Fig. 1C); however, the preference for phosphorylated over unphosphorylated substrates was unchanged (*14*). Thus, H59 appears to play an important role in catalyzing Pro isomerization or in binding the substrate Pro residue.

On the basis of amino acid preferences deduced for the six positions surrounding the pS-P motif for optimal Pin1 binding, we undertook a weighted screening of the SWISS-PROT sequence database (*15*). This scan revealed within the top 5% of high scores several potentially important mitotic phosphoprotein targets for Pin1. Many of these proteins contribute to regulation of the cell cycle, cytoskeletal or spindle structure, DNA replication, transcription, or RNA processing (see www.sciencemag.org/feature/data/974519.shl for supplementary data).

Several of the proteins, such as Rab4, Cdc25, and NIMA, undergo mitosis-specific phosphorylation (*3*, *16*). Cdc25 and NIMA have been previously shown to bind Pin1 in a phosphorylation-dependent manner (*7*). Other proteins identified in this search, however, had not been previously suspected of interacting with Pin1; a few were therefore further investigated as example cases (*7*, *17*). Rab4 and ribosomal S6 kinases were shown to interact with Pin1 specifically in extracts of mitotic, but not interphase, cells (Fig. 2, B and C). NIMA contains at least five predicted binding sites for Pin1, which may explain why Pin1 was originally isolated as a NIMA-interacting protein (*4*). Thus, Pin1 binds a wide functional range of mitotic phosphoproteins.

Differences in isomerase activity between Pin1 and other PPIases result from different organization of the X-P binding pocket. In all PPIases, a hydrophobic pocket sequesters the aliphatic Pro side chain (*5*); hence, the residues responsible for determining substrate preference must reside at the entrance to the Pro binding pocket. In Pin1 and its homologs (*4*, *18*), a cluster of basic residues coordinates the pS phosphate and determines substrate specificity. The absence of a basic pocket in the cyclophilins, FKBPs, and other members of the parvulin family of PPIases may explain their failure to catalyze isomerization of the pS/pT–P bond.

The specificity of Pin1 is consistent with the previous identification of Pin1 binding proteins (*7*) and also predicts other potential Pin1 substrates, some of which we have confirmed as targets of Pin1 in vitro. Furthermore, Pin1 and MPM-2 bind similar sequences and proteins and have similar mitosis inhibitory phenotypes (*7*), indicating that the wide conservation of MPM-2 epitopes across various species (*16*, *19*) can be explained by recognition

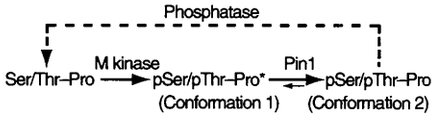

Fig. 3. A model for the Pin1-dependent regulation of mitosis-specific phosphoproteins that are phosphorylated by Cdc2 and other mitotic (M) kinases.

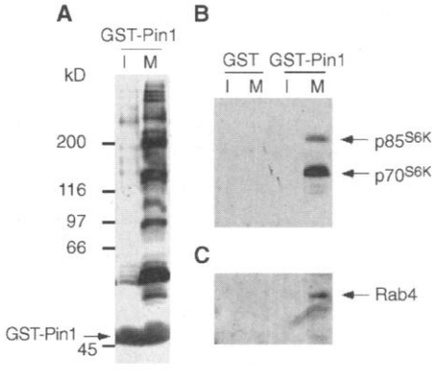

Fig. 2. Interaction between Pin1 and MPM-2 antigens or selected proteins predicted to bind Pin1 from a database search. (**A**) Interaction between Pin1 and MPM-2 antigens. After arrest at G_1-S (I) or mitosis (M), HeLa cells were harvested and lysed. The resulting soluble proteins were incubated with agarose beads containing GST-Pin1, and, after extensive washing, proteins associated with the beads were subjected to immunoblot analysis with MPM-2. Control GST beads did not precipitate any specific MPM-2 antigens, as described (*7*). The positions of molecular size standards (in kilodaltons) and GST-Pin1 (arrow) are indicated. (**B** and **C**) Interaction between Pin1 and S6 kinase (S6K) or Rab4. Beads containing GST-Pin1 or GST were incubated with extracts of HeLa cells in G_1-S or M phase and then washed, after which proteins associated with the beads were subjected to immunoblot analysis with antibodies to the COOH-terminal peptide of S6 kinases [which recognize both nuclear (p70) and cytoplasmic (p85) forms of the enzyme] (B) or with antibodies to Rab4 (C).

Table 3. Binding specificity of Pin1 and MPM-2. GST-Pin1 and MPM-2 were incubated with the pS-P–oriented degenerate peptide library H_2N-MAXXXpSPXXAKK, where X is any amino acid except Cys. After extensive washing, peptides bound to GST-Pin1 or MPM-2 were eluted and sequenced. Amino acids selected at each degenerate position are shown.

Ligand	Position							
	−3	−2	−1	0		+1	+2	+3
Pin1	W Y F	F I	Y R F W	pS	P	R F Y W	L I	X
MPM-2	Y F W	W F	F L I	pS	P	L I V F M	X	X

of this epitope by a highly conserved mitotic regulator, Pin1.

Our results suggest a two-step mechanism for mitotic regulation. Phosphorylation at specific S/T–P sites by mitotic kinases creates a binding site for Pin1, which, in turn, induces conformational changes by catalyzing prolyl isomerization (Fig. 3). Such local conformational changes could alter the activity of a phosphoprotein such as NIMA (*4*) or Cdc25 (*7*), its ability to interact with other proteins, or its degradation. In this manner, Pin1 would provide an additional posttranslational level of control, allowing the general increase in protein phosphorylation to result in the organized and programmed set of structural modifications that occur during mitosis. Given that inhibition of Pin1 induces mitotic arrest and apoptosis (*4*), this Pin1-mediated mechanism is a potential therapeutic target for cancer.

REFERENCES AND NOTES

1. P. Nurse, *Cell* **79**, 547 (1994); R. W. King, P. K. Jackson, M. W. Kirschner, *ibid.*, p. 563; T. R. Coleman and W. G. Dunphy, *Curr. Opin. Cell Biol.* **6**, 877 (1994).
2. E. A. Nigg, *Bioessays* **17**, 471 (1995).
3. R. Heald and F. McKeon, *Cell* **61**, 579 (1990); E. Bailly *et al.*, *Nature* **350**, 715 (1991); A. Blangy *et al.*, *Cell* **83**, 1159 (1995).
4. K. P. Lu, S. D. Hanes, T. Hunter, *Nature* **380**, 544 (1996); K. P. Lu and T. Hunter, *Cell* **81**, 413 (1995).
5. S. L. Schreiber, *Science* **251**, 283 (1991); G. Fischer, *Angew. Chem. Int. Ed. Engl.* **33**, 1415 (1994); F. X. Schmid, *Curr. Biol.* **5**, 993 (1995).
6. J. U. Rahfeld *et al.*, *FEBS Lett.* **352**, 180 (1994); *ibid.* **343**, 65 (1994); K. E. Rudd *et al.*, *Trends Biochem. Sci.* **20**, 12 (1995).
7. M. Shen, P. T. Stukenberg, M. W. Kirschner, K. P. Lu, in preparation.
8. The oriented peptide library approach [Z. Songyang *et al.*, *Cell* **72**, 767 (1993)] was used to screen for optimal peptides. All amino acids except Cys were incorporated in equimolar amounts at each degenerate position, yielding a total theoretical degeneracy for each library of 19^6 (4.7×10^7) distinct peptide sequences. GST-Pin1–conjugated beads, or MPM-2 antibody bound to protein G–conjugated beads, were incubated with the peptide library mixtures and then washed extensively. Bound peptides were eluted with 30% (v/v) acetic acid and sequenced.
9. R. Ranganathan, K. P. Lu, T. Hunter, J. P. Noel, *Cell* **89**, 875 (1997).
10. Chromogenic oligopeptides were synthesized [A. Bernhardt, M. Drewello, M. Schutkowski, *Int. J. Pept. Protein Res.* **50**, 143 (1997)], and their sequences were confirmed by nuclear magnetic resonance. Standard peptides were obtained from Bachem. PPIase activity was assayed, and the bimolecular rate constant (k_{cat}/K_m) was calculated according to the equation $k_{cat}/K_m = (k_{obs} - k_u)/[\text{PPIase}]$, where [PPIase] is the concentration of PPIase, k_u is the first-order rate constant for spontaneous cis-trans isomerization, and k_{obs} is the pseudo–first-order rate constant for cis-trans isomerization in the presence of PPIase, as described [G. Fischer, H. Bang, C. Mech, *Biomed. Biochim. Acta* **43**, 1101 (1984); J. L. Kofron *et al.*, *Biochemistry* **30**, 6127 (1991)]. The affinity of Pin1 for peptides was measured as described [M. Schutkowski, S. Wöllner, G. Fischer, *Biochemistry* **34**, 13016 (1995)].
11. M. B. Yaffe *et al.*, data not shown.
12. Molecular model-building was based on the coordinates of the Pin1 structure (*9*). The phosphate of pS in the modeled peptide was superimposed on the cocrystallizing sulfate ion in the original Pin1 structure, and Pro residue displacements were minimized with respect to the Ala-Pro ligand in the original Pin1 structure. Figures were made with the programs GRASP [A. Nicholls, K. Sharp, B. Honig, *Proteins* **11**, 281 (1991)], Molscript, and Raster3d.
13. Point mutations were introduced into Pin1 by polymerase chain reaction–based techniques and verified by DNA sequencing. The mutant proteins were expressed and purified as described (*4, 7*).
14. For Pin1, the ratio of k_{cat}/K_m values for the phosphorylated versus unphosphorylated substrates is 19,400/7, which is about equal to the ratio of 1120/<1 for the H59A mutant.
15. The protein sequence database was screened with the use of the program INDOVINATOR (S. Volinia, J. Lai, L. Cantley, in preparation), with an entropy-based weighting technique to score for relative information content at each amino acid position flanking the pS/pT–P motif with the quantitative peptide library results, which are shown qualitatively in Table 3 (see www.sciencemag.org/feature/data/974519.shl).
16. J. Kuang *et al.*, *Mol. Biol. Cell* **5**, 135 (1994); X. S. Ye *et al.*, *EMBO J.* **14**, 986 (1995); T. Izumi, D. H. Walker, J. L. Maller, *Mol. Biol. Cell* **3**, 927 (1992); A. Kumagai and W. G. Dunphy, *Science* **273**, 1377 (1996).
17. Lysates of interphase and mitotic HeLa cells were incubated with GST or GST-Pin1 beads and the precipitated proteins subjected to immunoblot analysis with various antibodies, as described (*7*). S6 kinase antibodies are from N. Terada (National Jewish Medical and Research Center) and Upstate Biotechnology and Rab4 antibodies are from Santa Cruz Biotechnology.
18. S. D. Hanes *et al.*, *Yeast* **5**, 55 (1989); R. Maleszka *et al.*, *Proc. Natl. Acad. Sci. U.S.A.* **93**, 447 (1996).
19. F. M. Davis *et al.*, *Proc. Natl. Acad. Sci. U.S.A.* **80**, 2926 (1983); J. M. Westendorf, P. N. Rao, L. Gerace, *ibid.* **91**, 714 (1994); S. Taagepera *et al.*, *Mol. Biol. Cell* **5**, 1243 (1994).

20. We thank M. Berne, A. Bernhardt, and B. Hökelmann for peptide synthesis and sequencing and N. Terada for the antibodies to S6 kinase. M.B.Y. is a Howard Hughes Physician-Scientist Fellow. Supported by Deutsche Forschungsgemeinschaft, Fonds der Chemischen Industrie, and Boehringer Ingelheim Stiftung to G.F., and NIH grants GM56203 to L.C.C. and GM56230 to K.P.L.

18 August 1997; accepted 3 November 1997

Mechanism of Transcription Through the Nucleosome by Eukaryotic RNA Polymerase

Vasily M. Studitsky,* George A. Kassavetis, E. Peter Geiduschek, Gary Felsenfeld†

Nucleosomes, the nucleohistone subunits of chromatin, are present on transcribed eukaryotic genes but do not prevent transcription. It is shown here that the large yeast RNA polymerase III transcribes through a single nucleosome. This takes place through a direct internal nucleosome transfer in which histones never leave the DNA template. During this process, the polymerase pauses with a pronounced periodicity of 10 to 11 base pairs, which is consistent with restricted rotation in the DNA loop formed during transfer. Transcription through nucleosomes by the eukaryotic enzyme and by much smaller prokaryotic RNA polymerases thus shares many features, reflecting an important property of nucleosomes.

Many transcribed genes are covered with nucleosomes (*1*, *2*), which raises the question of how the polymerase negotiates its obstructed passage (*3*, *4*). When the bacteriophage SP6 RNA polymerase transcribes through the nucleosome, the histone octamer steps around the polymerase by forming an intranucleosomal DNA loop (*5*). The looped intermediate causes intermittent pausing during the advance of the polymerase (*6*). Here we show that this mechanism is also relevant for eukaryotic RNA polymerases.

The ability of eukaryotic RNA polymerases to transcribe chromatin templates in vitro has been demonstrated (*7–13*), but the mechanism of transcription through the nucleosome remains obscure. Here we describe a new system for comparing transcription of identical nucleosomal templates by phage SP6 RNA polymerase and yeast RNA polymerase III (Pol III).

The template used for transcription was a 227–base pair (bp) Sac I–Nco I fragment (*5*) containing a positioned nucleosome and an SP6 promoter (Fig. 1A). DNA and nucleosomal templates labeled at the Nco I end were transcribed for different lengths of time (Fig. 1B). Elongation complexes were formed on DNA and nucleosomal templates with similar efficiency (on 25 to 30% of the templates). When elongation was continued for 5 min, the intensity of the low-mobility band was substantially reduced, which suggests that transcription on a majority of the templates was completed. Quantitative recovery of label from the elongation complexes in the nucleosomal band (naked DNA

V. M. Studitsky and G. Felsenfeld, Laboratory of Molecular Biology, National Institute of Diabetes and Digestive and Kidney Diseases, National Institutes of Health, Bethesda, MD 20892, USA.
G. A. Kassavetis and E. P. Geiduschek, Department of Biology and Center for Molecular Genetics, University of California, San Diego, La Jolla, CA 92093–0634, USA.

*Present address: Department of Biochemistry and Molecular Biology, Wayne State University School of Medicine, 540 East Canfield Avenue, Detroit, MI 48201, USA.
†To whom correspondence should be addressed.